

Ivan Mironyuk¹, Igor Mykytyn¹, Hanna Vasylyeva²

Structural and morphological properties of titanium dioxide nanoparticles doped by Boron atoms

¹Department of Chemistry, Vasyl Stefanyk Precarpathian National University,
57 Shevchenko Street, 76018 Ivano-Frankivsk, Ukraine, myrif555@gmail.com,

²Uzhhorod National University, 3 Narodna Square, 88000 Uzhhorod, Ukraine, h.v.vasylyeva@hotmail.com

The phase composition and morphology of boron-containing TiO₂ nanoparticles obtained by the sol-gel method were investigated. The solution of titanium aqua complex [Ti(OH)₆]³⁺ 3Cl⁻ was used as a precursor. Borate acid H₃BO₃ (promoter of the formation of rutile) was used as a modified reagent. A single-phase rutile TiO₂ was obtained at a concentration of borate acid in the reaction mixture, which causes the formation of a 0.5B-TiO₂ sample. The particles of 0.5B-TiO₂ samples were in the villi-form, with a diameter of 0.8-1.2 nm, and a length of 16-24 nm.

With an increase of the H₃BO₃ concentration in the reaction mixture, synthesized oxide materials (samples of 1.0B-TiO₂ and 1.5B-TiO₂) contain 70 % and 57% of anatase respectively, in addition to rutile phase. Meanwhile, anatase proto-particles with a diameter of 3-7 nm were combined into units of 60-100 nm in size in a two-phase composite mixture. Titanium-borate monodentate molecules Ti(OH)₃OB(OH)₂2H₂O were formed during the synthesis of the 0.5B-TiO₂ rutile sample. These molecules in the polycondensation process serve as centers of origin, growth, and crystallization of TiO₂ proto-particles. The interatomic distance of Ti-O in these particles is commensurate with the average length of the Ti-O – bond of TiO₆ rutile octahedra. During the polycondensation process, the distance of the Ti-O molecule-promoter was reproduced as a pattern in the following octahedra of rutile crystals.

Two types of titanium-borate molecules are formed in the reaction medium, during the synthesis of 1.0B-TiO₂ and 1.5B-TiO₂ samples. Molecules with a bidentate mononuclear structure Ti(OH)₂O₂BOH2H₂O were formed in addition to molecules with monodentate geometry of interatomic bonds. In molecules with a bidentate mononuclear structure, the interatomic distance of Ti-O is commensurate with the average length of the Ti-O –bond in the octahedra of the anatase phase. Therefore, titanium-borate molecules of the second type act as a promoter of the formation of the TiO₂ anatase phase.

Keywords: Titanium dioxide, Sol-gel, Borate acid, Anatase, Rutile.

Received 25 May 2022; Accepted 19 September 2022.

Introduction

Nanoparticle titanium dioxide, namely its polymorphic modifications of anatase and rutile, has unique physical and chemical properties. In particular, they are characterized by photoactivity and high adsorption capacity. Based on titanium dioxide, were made electrochemical photo-computers [1-4] and photovoltaic devices [5, 6]. Titanium dioxide possesses

high photocatalytic activity toward organic dyes and pharmaceuticals, for example, photocatalytic degradations of endocrine-disrupting compounds, 2,4-dichlorophenol (DCP) [7, 8]. Anatase modification of mesoporous TiO₂ with a chemically modified surface effectively adsorbs heavy metal cations as well as Sr (II) from the aquatic environment [9-12]. At the same time, mesoporous TiO₂ with a chemically modified surface selectively adsorbs Zr (IV) cations [13] from an acidic solution.

Currently known methods of synthesis of nanoparticle TiO₂ with a size of < 10 nm, based on the sol-gel method [14-16]. These methods allow getting mainly anatase modification of titanium dioxide. In the case of the necessity of obtaining rutile nanoparticles, sol-gel technologies have been combined with hydro- or solvo-thermal methods [17-20]. The main disadvantages of combined synthesis methods are their complexity, the large duration of the process, as well as the fact that the dimensions of rutile particles are large and exceed 20 nm.

This forces researchers to look for new ways to synthesize rutile, just using a simple sol-gel method. To obtain rutile with a small particle size by the sol-gel method, it is advisable to introduce metal cations into the solution of a titanium-containing precursor. Since metal cations can affect the course of structure-forming processes. According to [19] cations of Sn (II), Cd (II), Fe (II), Ni (II), Mn (II), Zn (II), Co (II), Cr (III), and Cu (II) are promoters of the formation of rutile TiO₂.

Other divalent cations, such as Ca (II), Sr (II), and Ba (II) (with a large ionic radius) stabilized the anatase modification of titanium dioxide during its synthesis. The stabilizing effect on TiO₂ anatase modification is also manifested by three-, tetra- valent cations, or cations with higher valence. The exception among three-valent elements is cations of B(III) – they support the formation of rutile. At present time, the direction of structure-forming processes in the liquid-phase synthesis of TiO₂ nanoparticles is not sufficiently studied. In particular, the mechanism of action of inorganic compounds – promoters introduced into the reaction medium for directing the crystallization process towards the formation of rutile or anatase – has not been established.

In this work, the phase formation was investigated during the sol-gel synthesis of titanium dioxide using a solution of titanium aqua complex [Ti(OH)₆]³⁺ 3Cl⁻ as a precursor, and borate acid H₃BO₃, as a promoter of the formation of rutile modification of TiO₂.

I. Synthesis of the experimental samples

The promoter of crystallization TiO₂, during the sol-gel synthesis of oxide material, was borate acid H₃BO₃. Borate acid, which contained 0.5, 1.0, or 1.5 wt.% of Boron, relate to the mass of TiO₂, was injected into the solution of [Ti(OH)₆]³⁺ 3Cl⁻ aqua-complex. The mixture of reagents was diluted with DI water to pH = 0.5-2.0, heated to a temperature of 60-70 °C, and kept heated for one hour. Very small particles of oxide material were formed in the volume of the reaction mixture during the heating. The medium became cloudy and acquired a whitish tint.

After the finish of the heating process, NaOH was injected into the dispersion and the pH of the reaction medium was increased to ~ 7. Synthesized particles were removed from the reaction medium using a vacuum filter, laundered from Na⁺ and Cl⁻ by distilled water, and dried at a temperature of 120-140°C.

Synthesized samples of titanium dioxide containing 0.5, 1.0, and 1.5% of Boron atoms are marked respectively 0.5B-TiO₂; 1.0B-TiO₂, and 1.5B-TiO₂, and the bare

sample that does not contain in its structure Boron is marked as a-TiO₂ in the text of the present manuscript.

II. Methods of the investigations of the TiO₂ property

2.1. XRD

Studies of X-ray diffraction of bare a-TiO₂ and Boron-containing TiO₂ samples were performed using the STOE STADIP X-ray powder diffractometer in the radiation of the Cu anode. Since the CuKα line is usually used as the x-ray source in powder diffractometry. The focus of the rays was carried out according to the configuration of the Bragg-Brentano.

Rietveld analysis of recorded diffractograms was carried out using SHELXL-97 software [21], in which simulation reproduction of the form of areas of coherent dispersion (ACD) was carried out using the Rietveld method [22]. Rietveld refinement allows determinations of positional and thermal parameters from powder data, even when the diffraction peaks are not well separated in the recorded pattern.

The main parameters of TiO₆ octahedra, namely the Ti-O distance in the equatorial and axial plane, are calculated by direct method and specified by the method of least squares by minimizing the sum of the squares of the residuals (a residual being: the difference between an observed value, and the fitted value provided by a model) in full-time anisotropic approximation.

2.2. TEM imaging

The morphology of the sample was investigated by transmission electron microscope (TEM). Images of bare a-TiO₂ and Boron-contained samples nanoparticles were obtained using the transmission electron microscope (TEM) LSM 2100F. Accelerating the voltage during TEM operation was 200 kV.

2.3. IR-spectrometry

Infrared spectra (IR spectra) of TiO₂ samples were recorded on the SPECORD M80 spectrophotometer in the range of 2000-400 cm⁻¹. The samples with the weight of 4 mg were mixed with KBr at a ratio of 1:100, crushed in a vibration mill for 10 minutes and the spectrum was recorded. The prepared samples of the mixture were formed by pressing a transparent plate with a size of 20×5 mm².

2.4. Nitrogen adsorption/desorption isotherms

The morphological characteristics of TiO₂ samples, namely their specific surface area, pore volume, and pore size distribution, were calculated by the low-temperature Nitrogen adsorption/desorption isotherms. Adsorption studies were conducted at the boiling point of liquid Nitrogen (T = 77K) on the Quantachrome Autosorb automatic equipment (Nova 2200e).

The bare a-TiO₂ and Boron-contained samples of TiO₂ were calcined in a vacuum at a temperature of 180°C for 24 hours before measurement. After the measurement, the morphological characteristics of TiO₂ samples were calculated using density functional theory (DFT) [23].

III. Results and discussion

3.1. The phase composition of the investigated samples

X – radiation diffractograms of experimental samples 0.5B-TiO₂, 1.0B-TiO₂, 1.5B-TiO₂, as well as a-TiO₂ are shown in Fig.1.

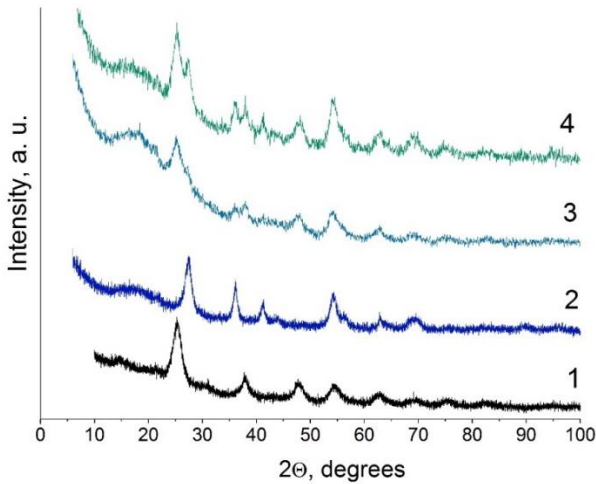


Fig.1. XRD spectra of the samples: 1 – a-TiO₂; 2 – 0.5 B-TiO₂; 3 – 1.0 B-TiO₂; 4 – 1.5 B-TiO₂.

The phase composition of these samples and the structural characteristics of their crystalline components are given in Table 1.

The bare sample a-TiO₂ contains a single phase – anatase (spatial group $I_{41/amd}$) (Fig.2 (a)). The introduction of 0.5% of the B (III) cations into the structure of titanium dioxide (sample 0.5B-TiO₂, TEM image is shown in Fig. 2 (b)) leads to the formation of a single-phase material – rutile (spatial group $P_{42/mnm}$).

However, with an increase in the B atoms amount in samples 1.0B-TiO₂ and 1.5B-TiO₂, titanium dioxide samples become two-phase compounds. They include rutile and anatase modifications of TiO₂, respectively, in the amount of 30 and 43 wt. % of rutile and 70 and 57 wt. % of anatase.

The dimensions of the coherent scattering domains of the a-TiO₂ anatase sample (average apparent crystalline size) are ~ 2.9 nm, according to the determination of the reflex (101) of the tetragonal lattice. In the rutile sample of 0.5B-TiO₂, the sizes of domains were determined by reflex (110), their size is close to ~ 5.1 nm.

The small pores in the rutile sample are the gaps between the very thin needle-shaped “villi” collected in “sheaves”, as can be seen in Fig. 2 (b)

In two-phase samples of 1.0B-TiO₂ and 1.5B-TiO₂, rutile domains are 6.1 nm and 5.7 nm, respectively; and anatase domains are 3.5 nm and 3.9 nm respectively in 1.0B-TiO₂ and 1.5B-TiO₂. It had been noted, that the rutile domains in two-phase samples are larger than the rutile domains in the single-phase sample, and the anatase domains in these samples are close in size.

The calculations show that the interatomic distance of Ti-O in the equatorial plane of the TiO₆ octahedrons is 0.19466 nm, and in the axial - 0.19924 nm in the 0.5B-TiO₂ rutile sample.

Table 1

The phase composition and the structural characteristics of the bare a-TiO₂ and Boron-contained TiO₂ samples.

Sample	Anatase						Rutile					
	Content, %	a, Å	c, Å	Ti-O (axial) Å	Ti-O (plane) Å	Particle size, nm	Content, %	a, nm	c, nm	Ti-O (axial) Å	Ti-O (plane) Å	Particle size, nm
a-TiO ₂	100	3.784	9.513	1.9787	1.9337	2.9±1.4	–	–	–	–	–	–
0.5B-TiO ₂	–	–	–	–	–	–	100	4.610	2.955	1.9924	1.9466	5.1
1.0B-TiO ₂	70±4	3.796	9.496	1.9752	1.9395	3.5	30±3	4.637	2.946	2.0040	1.9480	6.1
1.5B-TiO ₂	57±2	3.787	9.499	1.9758	1.9351	3.9	43±2	4.602	2.958	1.9889	1.9463	5.7

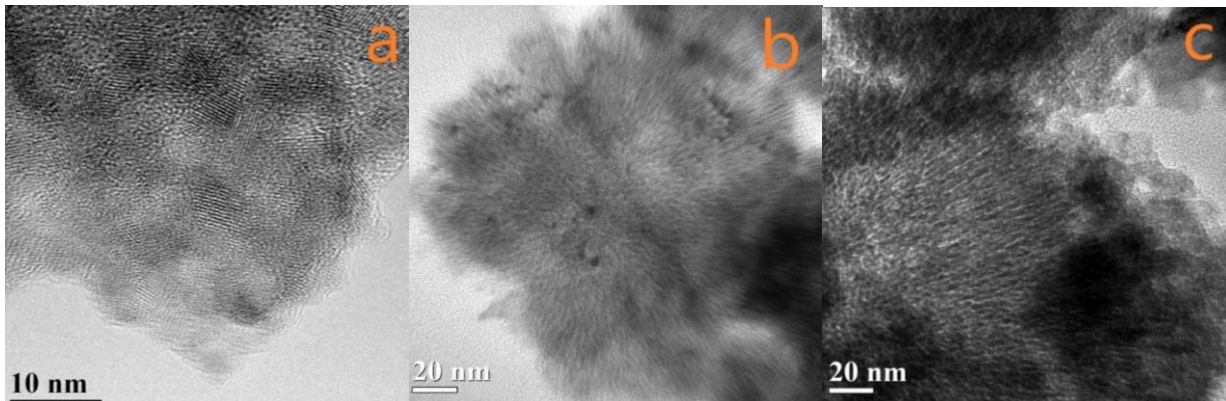


Fig. 2. TEM image of the titanium dioxide particles: (a) bare anatase sample a-TiO₂, (b) rutile sample 0.5 B-TiO₂ and (c) anatase-rutile sample 1.0 B-TiO₂.

In the octahedrons of the a-TiO₂ anatase sample, the length of the Ti-O bond is 0.19337 nm in the equatorial plane, and - 0.19787 nm in the axial plane. The same proportions relative to the length of the Ti-O bonds are maintained in the anatase and rutile of two-phase samples.

3.2. IR –studies of the a-TiO₂ and TiO₂ doped by Boron atoms

IR spectra of the samples, which are shown in Fig. 3., confirm their phase composition, as well as the different coordination states of atom B in the structure of anatase and rutile. Oscillation mods of TiO₆ octahedrons are manifested by absorption bands in the range of 2000-400 cm⁻¹ in the IR spectra of TiO₂ (Fig. 3).

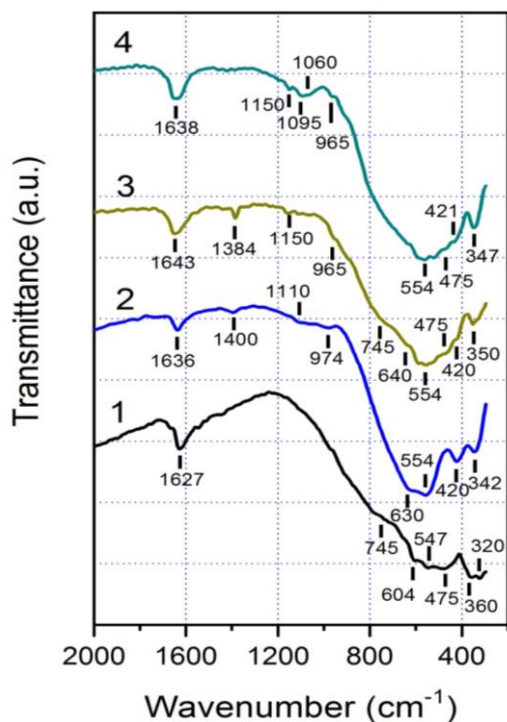


Fig.3. IR spectra of the samples: 1 – a- TiO₂; 2 – 0.5 B-TiO₂; 3 – 1.0 B-TiO₂; 4 – 1.5 B-TiO₂.

In the spectrum of the a-TiO₂ sample (Fig. 3, spectrum 1), bands of degenerate oscillations E_v octahedra with peaks at 604 cm⁻¹; 547 cm⁻¹, and 475 cm⁻¹ are recorded [24]. Symmetrical oscillations of A_{2u} anatase octahedra in the spectrum of a-TiO₂ bare sample correspond to the bands 745 cm⁻¹ and 369-320 cm⁻¹. Degenerate vibrations of E_v rutile octahedrons in the spectrum of the sample 0.5B-TiO₂ (Fig. 3, spectrum 2) are manifested by absorption peaks at 630 cm⁻¹, 554 cm⁻¹, and 420 cm⁻¹ [25, 26].

The high-frequency component of A_{2u} oscillation bands in the spectrum of this sample is not registered, but the low-frequency component of this band belongs to the strip at 342 cm⁻¹. The larger parameters of the rutile octahedron TiO₆ compared to the parameters of the octahedron of anatase, cause the displacement of the bands of oscillating rutile mods in the direction of reducing their frequency characteristics.

In the IR spectra of two-phase samples 1.0B-TiO₂ and 1.5B-TiO₂ (Fig. 3, spectra 3 and 4), bands of both rutile

and anatase are recorded. It had been noted, that the frequency characteristics of the oscillation mods of each of these phases are the same as the frequency of oscillation mods of single-phase samples.

The surface of all TiO₂ samples is hydrated. This is confirmed by the band at 1643-1627 cm⁻¹, which belongs to the deformation oscillations of O-H groups, in adsorbed H₂O molecules [27].

The structural cell of the crystal lattice of borate acid is the group of BO₃ in the form of an equilateral triangle. The symmetry of the lattice belongs to the point group C_{3v}.

In the IR spectra of borate acid, the mode of A₂ symmetric oscillations with a frequency of ν₃ = 1060 cm⁻¹ is well manifested, as well as the band of degenerate E¹ asymmetric oscillations (ν₇ = 1440 cm⁻¹) and the twice degenerate E¹¹ asymmetric oscillations (ν₉ = 1190 cm⁻¹) [28].

In the spectrum of the 0.5B-TiO₂ sample (Fig. 3, spectrum 2), weak bands of 1400 cm⁻¹, 1110 cm⁻¹, and 974 cm⁻¹ are recorded, which are attributed to fluctuations in BO₃ groupings.

The first two stripes we attribute to the degenerate asymmetrical fluctuations of bands E¹ and E¹¹, and in the third band, similar to the authors [29] we attribute asymmetric deformation oscillation grouping B-OH. Thus, the results of studies show that atoms B, incorporated into the rutile TiO₂, forms a grouping of BO₃ with the structure of the triangle. Hydroxyl groups in these groups certify their location in the surface layer of the TiO₂ particles.

Boron atoms are in tetrahedral coordination concerning oxygen atoms in anatase TiO₂. Tetrahedral anion BO₄⁻ in IR-spectra is manifested by stripes of 1150 cm⁻¹ and 965 cm⁻¹.

The 1.0B-TiO₂ and 1.5B-TiO₂ samples are two-phase. They contain crystallites of both anatase and rutile. In the rutile phase, these samples incorporated grouping BO₃ with the structure of the triangle. In spectra, they own absorption bands of 1384 cm⁻¹ and 1035 cm⁻¹.

According to [30] in the spectrum of tetrahedral anion B(OH)₄⁻ two characteristic bands around 1170 cm⁻¹ (deformation oscillations of B-OH group) and 955 cm⁻¹ (longitudinal asymmetric oscillations of B-OH group) are recorded. Groups of BO₃ in the rutile phase and anionic groups of BO₄⁻ in the anatase phase indicate the different nature of titanium-borate molecules that promote the formation of crystalline phases.

3.3. Morphology of investigated samples

Adsorption/desorption isotherms of N₂ molecules of bare a-TiO₂ (unmodified) and boron-modified samples of titanium dioxide are shown in Fig. 4. And are given in Table 2. The parameters of their porous structure calculated by these isotherms are given in Table 2, and the pore size and volume distribution are shown in Fig. 4.

As can be seen, the introduction of the B (III) cations into the lattice of oxide material affects not only the crystalline structure but also the morphology of the titanium dioxide. In particular, the specific surface area of the rutile sample 0.5B-TiO₂ is 152 m²g⁻¹ and is much lower compared to other samples. The volume of pores in it is also not high – 0.116 cm³g⁻¹.

Table 2

Textural characteristics (specific surface area, pore volume).						
Sample	S_{BET} (m^2g^{-1})	S_{micro} (m^2g^{-1})	S_{meso} , (m^2g^{-1})	V_p , (cm^3g^{-1})	V_{micro} (cm^3g^{-1})	V_{meso} (cm^3g^{-1})
a-TiO ₂	239.4	100.5	138.9	0.1519	0.054	0.098
0.5B-TiO ₂	151.6	81.73	69.87	0.1158	0.04175	0.07405
1.0B-TiO ₂	316.1	14.25	301.85	0.2918	0.00661	0.28519
1.5B-TiO ₂	254.1	-	254.1	0.3442	-	0.3442

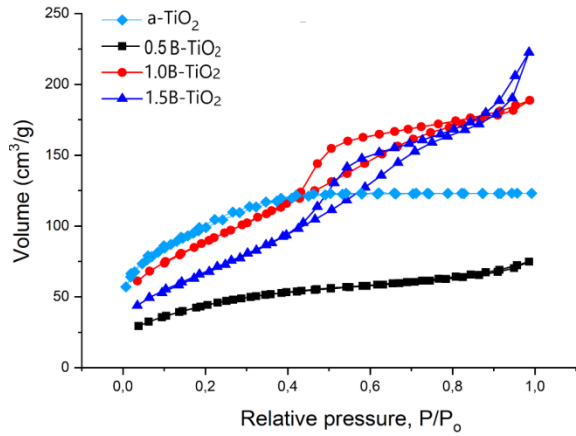


Fig.4. Adsorption/desorption isotherms of N₂ molecules with bare a-TiO₂ and boron-contained samples.

The specific surface of the micropore is 81.7 m^2g^{-1} and exceeds the specific surface of the mesopores, which is equal to 69.9 m^2g^{-1} . According to the distribution of pores by size (Fig. 5), in the single-phase rutile sample pores with a radius of 1.3 nm are dominated.

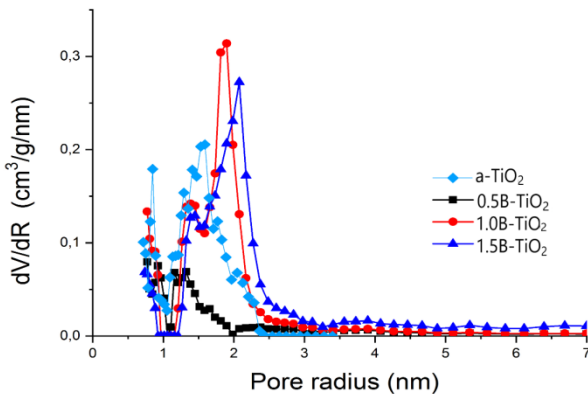


Fig.5. Distribution of pores by their size (radius) in the bare a-TiO₂ and Boron-containing samples of TiO₂.

In two-phase samples of 1.0B-TiO₂ and 1.5B-TiO₂, the main number of pores has a radius of 1.8 nm and 2.1 nm, respectively.

The specific surface of the two-phase samples 1.0B-TiO₂ and 1.5B-TiO₂ is respectively 316 m^2g^{-1} and 254 m^2g^{-1} and exceeds the specific surface of single-phase samples - rutile 0.5B-TiO₂ and anatase a-TiO₂.

As the anatase phase increases in the 1.5B-TiO₂ sample, its specific surface decreases. The volume of pores of two-phase samples is three times higher than the volume of pores of a single-phase rutile sample.

Single-phase and two-phase mesoporous boron-doped TiO₂ synthesized by the sol-gel method can reach ion-exchange properties. This is indicated by their special structural and morphological characteristics. According to [29-33] the introduction of B atoms into the structure of TiO₂ contributes to an increase in the photoactivity of the oxide material.

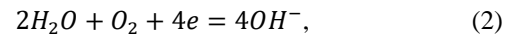
3.4. Formation of titanium-borate molecules and their effect on crystallization of titanium dioxide

Heating the precursor solution mixture [Ti(OH)₂]³⁺ 3Cl and borate acid H₃BO₃, which corresponds to the stoichiometry of the 0.5B-TiO₂ sample, causes the following reactions.

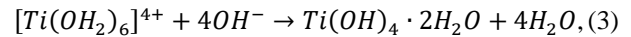
Oxidation of Ti³⁺ cations to Ti⁴⁺ is occurring:



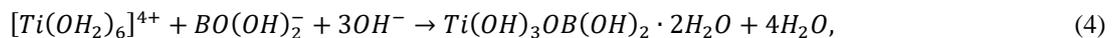
The released electrons restore H₂O molecules, which in turn causes the formation of OH⁻ anions:



The hydrolysis of cations of the aqua complex occurs by OH⁻ anions, and this leads to the formation of molecules of titanium hydroxide:



Part of the cations [Ti(OH)₂]⁴⁺ attaches borate acid anions:



Since the electronegativity of atoms B is 2.04 and exceeds the electronegativity of Ti atoms (1.54), the formed titanium-borate molecules Ti(OH)₃OB(OH)₂·2H₂O are the first to be involved in the polycondensation process with Ti(OH)₄·2H₂O molecules.

The higher electronegativity of atom B concerning the

electronegativity of the atom Ti causes the displacement of the electron density in the bridges of the Ti-O-B in the titanium-borate molecule toward the Boron atom.

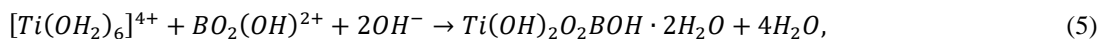
This causes the lengthening of the interatomic distance of Ti-O in the titanium-borate molecule.

Titanium-borate molecules act as centers of origin and growth of TiO₂ proto-particles, in the polycondensation

process. The interatomic distance of the Ti-O titanium-borate molecule is reproduced in all TiO_6 octahedra of the formed TiO_2 particles. Since the distance of Ti-O in the titanium-borate monodentate molecule is equal to the average length of the Ti-O bond of rutile, therefore, the polycondensation process leads to the formation of a rutile phase. Therefore, the reason for the rutile phase formation in the study sample 0.5B- TiO_2 is titanium-borate molecules with monodentate grouping B-O-Ti in which the length of the Ti-O bond is commensurate with the average interatomic distance of Ti-O in the octahedra TiO_6

rutile.

The more significant chemical potential of borate acid molecules in the reaction mixture, during the synthesis of prototypes 1.0B- TiO_2 and 1.5B- TiO_2 , causes the formation of two types of titanium-borate molecules. In addition to molecules with monodentate geometry of bonds $\text{Ti}(\text{OH})_3\text{OB}(\text{OH})_2\cdot 2\text{H}_2\text{O}$, molecules with bidentate mononuclear structure $\text{Ti}(\text{OH})_2\text{O}_2\text{BOH}\cdot 2\text{H}_2\text{O}$ by the reaction are formed:



The bidentate geometry of the bonds in the Boron-doped titanium dioxide molecule makes it impossible to elongate the interatomic distance of Ti-O, due to the presence of two Oxygen atoms between atoms B and Ti. In bidentate titanium-borate molecules, the interatomic distance of the Ti-O bond is commensurate with the interatomic distance of this bond in the anatase octahedron.

In this regard, molecules of the $\text{Ti}(\text{OH})_2\text{O}_2\text{BOH}\cdot 2\text{H}_2\text{O}$ are promoters of the formation of the anatase phase of TiO_2 . Therefore, in the samples of 1.0 B- TiO_2 and 1.5 B- TiO_2 , in addition to rutile in the amount of 30 wt. % and 43 wt. %, the certain mass of anatase 70 wt. % and 57 wt. % is contained.

Conclusions

The sol-gel synthesis of titanium dioxide nanoparticles using the aqua complex of the precursor $[\text{Ti}(\text{OH}_2)_6]^{3+}\cdot 3\text{Cl}^-$ and borate acid H_3BO_3 , as a modified reagent, leads to the introduction of B atoms into the structure of TiO_2 and changes in its phase composition.

At a low concentration of borate acid, a single-phase rutile oxide material (sample 0.5 B- TiO_2) is formed in the reaction medium. Needle-shaped rutile "villi" with a diameter of 0.8-1.2 nm and a length of 16-24 nm form mesoporous associates with an average pore size of 1.3 nm.

TiO_2 is formed with a higher content of B atoms (samples 1.0B- TiO_2 and 1.5B- TiO_2), with an increase in the H_3BO_3 concentration in the reaction mixture. Synthesized samples are two-phase. In addition to rutile, they contain, respectively, 30 % and 43 % of the mass of anatase. Pores in synthesized two-phase material have a

size of 1.8 nm and 2.1 nm, respectively.

The promoter of rutile formation during liquid-phase synthesis of TiO_2 is titanium-borate monodentate molecules $\text{Ti}(\text{OH})_3\text{OB}(\text{OH})_2\cdot 2\text{H}_2\text{O}$. The peculiarity of Boron-doped TiO_2 molecules is that the interatomic distance of Ti-O in them is commensurate with the average bond length in the octahedrons of rutile. Titanium-borate molecules serve as centers of origin, growth, and crystallization of TiO_2 proto-particles in the polycondensation process. The length of the Ti-O bond of these molecules is reproduced in the octahedra of TiO_2 nanocrystallites. The Ti-O distance in the titanium-borate molecule is the pattern by which the structure of the rutile solid phase is formed.

During the synthesis of the samples of 1.0B- TiO_2 and 1.5B- TiO_2 , two types of titanium-borate molecules are formed in the reaction medium. In addition to molecules with monodentate geometry of interatomic bonds, molecules with a bidentate mononuclear structure $\text{Ti}(\text{OH})_2\text{O}_2\text{BOH}\cdot 2\text{H}_2\text{O}$ are formed.

In a $\text{Ti}(\text{OH})_2\text{O}_2\text{BOH}\cdot 2\text{H}_2\text{O}$ molecule, the interatomic distance of Ti-O is commensurate with the average length of the Ti-O bond in the octahedra of anatase phase. In this regard, Boron-doped TiO_2 molecules of the second type cause the formation of the anatase phase of TiO_2 .

Mironyuk Ivan – Head of Department of Chemistry, Vasyl Stefanyk Precarpathian National University;

Mykytyn Igor – Associated professor, Department of Chemistry, Vasyl Stefanyk Precarpathian National University;

Vasylyeva Hanna – Associated professor, Department of Theoretical Physics, Uzhgorod National University.

- [1] C.Y. Kwong, W.C.H. Choy, A.B. Djuricic, P.C. Chui, K.W. Cheng, W.K. Chan. Poly(3-hexylthiophene): TiO_2 nanocomposites for solar cell applications, *Nanotechnology*, 15, 1156 (2004).
- [2] H.Z. Yu, J.C. Liu, J.B. Peng. Photovoltaic cells with TiO_2 nanocrystals and conjugated polymer composites, *Chin. Phys. Lett.*, 25, 3013 (2008).
- [3] J. Zhao, J. Yao, Y. Zhang, M. Guli, L. Xiao, Effect on thermal treatment on TiO_2 nanorod electrodes prepared by the solvothermal method for dye-sensitized solar cells: Surface reconfiguration and improved electron transport, *J. Power Sources*, 255, 16 (2014).
- [4] X.Li, S.M. Dai, P. Zhu, L.L. Deng, S.Y. Xie, Q. Cui, H. Chen, N. Wang, H. Lin, Efficient perovskite solar cells depending on TiO_2 nanorod arrays, *ACS Appl. Mater. Interfaces*. 8, 21358 (2016).

- [5] Imran Ali, Mohd Suhait, Zied A. Allothman and Abdulrahman Alwarthan. Recent advances in syntheses, properties, and application of TiO₂ nanostructures. *RSC Adv.* 8, 30125, (2018).
- [6] Sadhana S. Rayalu, Deepa Jose, Meenal V. Joshi, Priti A. Mangrulkar, Khadga Shrestha, Kenneth Klabunde. Photocatalytic water splitting on Au/TiO₂ nanocomposites synthesized through various routes: Enhancement photocatalytic activity due to SPR effect. *Applied Catalysis B: Environmental* 142, 684 (2013).
- [7] Esra Bilgin Simsek, Solvothermal synthesized boron-doped TiO₂ catalysts: Photocatalytic degradation of endocrine-disrupting compounds and pharmaceuticals under visible light irradiation, *Applied Catalysis B: Environmental*, 200, 309 (2017); <https://doi.org/10.1016/j.apcatb.2016.07.016>.
- [8] Kolade Augustine Oyekan, Maarten Van de Put, Sabyasachi Tiwari, Carole Rossi, Alain Esteve, William Vandenberghe, Re-examining the role of subsurface oxygen vacancies in the dissociation of H₂O molecules on anatase TiO₂, *Applied Surface Science*, 594, (2022); <https://doi.org/10.1016/j.apsusc.2022.153452>.
- [9] I. Mironyuk, T. Tatarchuk, H. Vasylyeva, V. Gun'ko, I. Mykytyn, Effects of chemisorbed arsenate groups on the mesoporous titania morphology and enhanced adsorption properties towards Sr (II) cations, *J. of Molecular Liquids*, 282, 587 (2019). <https://doi:10.1016/J.MOLLIQ.2019.03.026>.
- [10] I. Mironyuk, T. Tatarchuk, Mu. Naushad, H. Vasylyeva, I. Mykytyn, Adsorption of Sr (II) cations onto phosphate mesoporous titanium dioxide: mechanism, isotherm, and kinetics studies. *Journal of Environmental Chemical Engineering* 7(6), 103430 (2019). <https://www.doi.org/10.1016/j.jece.2019.103430>.
- [11] I. Mironyuk, T. Tatarchuk, Mu. Naushad, H. Vasylyeva, I. Mykytyn, Highly Efficient Adsorption Of Strontium Ions By Carbonated Mesoporous TiO₂. *J. of Molecular Liquids*, 285, 742 (2019). <https://www.doi.org/10.1016/j.molliq.2019.04.111>.
- [12] H. Vasylyeva, I. Mironyuk, I. Mykytyn, Kh. Savka, Equilibrium studies of yttrium adsorption from aqueous solutions by titanium dioxide, *Applied Radiation and Isotopes*, 168, (2021); <https://doi.org/10.1016/j.apradiso.2020.109473>.
- [13] H. Vasylyeva, I. Mironyuk, M. Strilchuk, I. Maliuk, V. Tryshyn. A new way to ensure selective zirconium ion adsorption. *Radiochimica Acta*, 109(12), (2021); <https://doi.org/10.1515/ract-2021-1083>.
- [14] P. Pookmanee and S. Phanichphant. Titanium dioxide powder prepared by a sol-gel method, *Journal of Ceramic Processing Research*, 10(2), 167 (2009).
- [15] R.F. de Farias. A new experimental procedure to obtain titania powders as anatase phase by a sol-gel process, *Quim. Nova*, 25(6), 1027 (2002).
- [16] G. Li, L. Li, J.B. Goates, and B.F. Woodfield. Grain-growth kinetics of rutile TiO₂ nanocrystals under hydrothermal conditions, *J. Mater. Res.*, 18(11), 2664 (2003).
- [17] G.Q. Guo, J.K. Whitesell, M.A. Fox. Synthesis of TiO₂ photocatalysts in supercritical CO₂ via a non-hydrolytic route, *J. Phys. Chem. B*, 109, 18781 (2005).
- [18] M. Niederberger, M.H. Bartl, G.D. Stucky. Benzyl alcohol and titanium tetrachlorides a versatile reaction system for the nonaqueous and low-temperature preparation of crystalline and luminescent titania nanoparticles, *Chem. Mater.*, 14(10), 4364 (2002).
- [19] Dorian A. H. Hanaor, Charles C. Sorrell. Review of the anatase to rutile phase transformation. *J. Mater. Sci.*, 46, 855 (2011).
- [20] Niu Pingping, Wu Guanghui, Chen Pinghua, et al., Optimization of Boron Doped TiO₂ as an Efficient Visible Light-Driven Photocatalyst for Organic Dye Degradation With High Reusability. *Frontiers in Chemistry*, 8 (2020); <https://www.frontiersin.org/article/10.3389/fchem.2020.00172>
- [21] G.M. Sheldrick. SHELXL-97. Program for the refinement of crystal structures. Göttingen: Univ. Göttingen, Germany (1997).
- [22] Rodriguez-Carvajal. FULLPROF: A program for Rietveld refinement and pattern matching analysis// Abstracts of the satellite meeting on powder diffraction of the XV Congress of the IUCr, Toulouse, France. 127 p. (1990).
- [23] V.M. Gun'ko, V.V. Turov, Nuclear magnetic resonance studies of interfacial phenomena, CRC Press, Boca Raton, 2013.
- [24] T. Posch, F. Kerschbaum, D. Fabian, et al. Infrared properties of solid titanium oxides: exploring potential primary dust condensates, *Astrophys. J. Suppl. Ser.*, 149, 437 (2003).
- [25] M. Ocaña, V. Fornés, J.V. García Ramos, C.J. Serna. Factors affecting the infrared and Raman spectra of rutile powders, *Journal of Solid State Chemistry*, 75 (2), 364 (1988).
- [26] G.-W. Peng, S.-K. Chen, H.-S. Liu. Infrared Absorption Spectra and Their Correlation with the Ti-O Bond Length Variations for TiO₂(Rutile), Na-Titanates, and Na-Titanosilicate (Natisite, Na₂TiOSiO₄), *Appl. Spectrosc.*, 49, 1646 (1995).
- [27] L.I. Myronyuk, I.F. Myronyuk, V.L. Chelyadyn, V.M. Sachko, M.A. Nazarkovsky, R. Leboda, J. Skubiszewska-Zie, V.M. Gun'ko. Structural and morphological features of crystalline nano titania synthesized in different aqueous media. *Chemical Physics Letters* 583, 103, (2013).
- [28] K.M. Mackay, R.A. Mackay, W. Henderson, *Introduction to modern inorganic chemistry*, 5th ed., Blackie Academic and professional, and imprint of Chapman and Hall, 2-6 Boundary Row, London, UK (1996).
- [29] G. Lefèvre, In situ Fourier-transform infrared spectroscopy studies of inorganic ions adsorption on metal oxides and hydroxides, *Adv. Colloid. Interfac.* 107, 109 (2004); <https://doi.org/10.1016/j.cis.2003.11.002>.

- [30] X.-S. Liu, Chapter 6 - Inorganic Photochemical Synthesis, Editor(s): Ruren Xu, Yan Xu, Modern Inorganic Synthetic Chemistry (Second Edition), Elsevier, (2017) 143-165. <https://doi.org/10.1016/B978-0-444-63591-4.00006-9>
- [31] Yongqiang Yang, Yuyang Kang, Gang Liu, Hui-Ming Cheng, Homogeneous boron doping in a TiO₂ shell supported on a TiB₂ core for enhanced photocatalytic water oxidation, Chinese Journal of Catalysis, 39(3), 431 (2018); [https://doi.org/10.1016/S1872-2067\(18\)63043-8](https://doi.org/10.1016/S1872-2067(18)63043-8).
- [32] Kui Zhang, Xiangdong Wang, Tianou He, Xiaoling Guo, Yaming Feng, Preparation and photocatalytic activity of B–N co-doped mesoporous TiO₂, Powder Technology, 253, 608 (2014); <https://doi.org/10.1016/j.powtec.2013.12.024>.
- [33] E. Grabowska, A. Zaleska, J.W. Sobczak, M. Gazda, J. Hupka, Boron-doped TiO₂ Characteristics and photoactivity under visible light, Procedia Chemistry, 1(2), 1553 (2009); <https://doi.org/10.1016/j.proche.2009.11.003>.

Іван Миронюк¹, Ігор Микитин¹, Ганна Васильєва²

Структурно-морфологічні властивості наночастинкового діоксиду титану допованого атомами Бору

¹Кафедра хімії, Прикарпатський національний університет ім. В. Стефаника, вул. Шевченка, 57, 76018 Івано-Франківськ, Україна, myrif555@gmail.com

²Кафедра теоретичної фізики, Ужгородський національний університет, вул. Університетська, 88000, Ужгород, Україна, h.v.vasylyeva@hotmail.com

Досліджували фазовий склад та морфологію наночастинкових борвмісних зразків TiO₂, одержаних золь-гель методом, з використанням як прекурсора розчину титанового аквакомплексу [Ti(OH)₆]³⁺ 3Cl⁻ та модифікуючого реагента, промотора утворення рутилу боратної кислоти H₃BO₃.

При концентрації боратної кислоти в реакційному середовищі, що спричинює утворення дослідного зразка 0.5В-TiO₂, одержується однофазний рутильний TiO₂, в якому частинки мають форму ворсинок, їх діаметр становить 0.8-1.2 нм, а довжина 16-24 нм. При більшій концентрації H₃BO₃, синтезовані оксидні матеріали (дослідні зразки 1.0В-TiO₂, 1.5В-TiO₂) містять, крім рутилу, відповідно 70 і 57 мас.% анатазу. В двохфазній композиційній суміші проточастинки анатазу діаметром 3-7 нм об'єднані в агрегати розміром 60-100 нм. В ході синтезу рутильного зразка 0.5В-TiO₂ утворюються титаноборатні монодентатні молекули Ti(OH)₃OB(OH)₂2H₂O. Ці молекули в поліконденсаційному процесі служать центрами зародження, зростання і кристалізації проточастинок TiO₂. В них міжатомна відстань Ti-O співрозмірна з середньою довжиною Ti-O – зв'язку октаедрів TiO₆ рутилу. В ході поліконденсаційного процесу відстань Ti-O молекули-промотора, як шаблон відтворюється в октаедрах кристалітів рутилу. Під час синтезу зразків 1.0В-TiO₂ і 1.5В-TiO₂ в реакційному середовищі утворюються два типи титаноборатних молекул. Крім молекул із монодентантною геометрією міжатомних зв'язків, утворюються молекули з бідентантною мононуклеарною структурою Ti(OH)₂O₂BOH2H₂O. У цій молекулі міжатомна відстань Ti-O співрозмірна з середньою довжиною Ti-O – зв'язку в октаедрах анатазної фази. У зв'язку з цим, титаноборатні молекули другого типу є промотором утворення анатазної фази TiO₂.

Ключові слова: Діоксид титану, Золь-гель метод, Анатаз, Рутил.